Stellar activity as a tracer of moving groups[*]

F. Murgas[1], J. S. Jenkins[2,3], P. Rojo[2], H.R.A Jones[3], and D.J. Pinfield[3]

[1] Instituto de Astrofísica de Canarias (IAC), E-38205 La Laguna, Tenerife, Spain
 e-mail: murgas@iac.es
[2] Departamento de Astronomía, Universidad de Chile, Casilla Postal 36D, Santiago, Chile
[3] Center for Astrophysics Research, University of Hertfordshire, College Lane, Hatfield, Herts, UK, AL10 9AB

ABSTRACT

We present the results of a study of the stellar activity in the solar neighborhood using complete kinematics (galactocentric velocities U,V,W) and the chromospheric activity index $\log R'_{HK}$. We analyzed the average activity level near the centers of known moving groups using a sample of 2529 stars and found that the stars near these associations tend to be more active than field stars. This supports the hypothesis that these structures, or at least a significant part of them, are composed of kinematically bound, young stars. We confirmed our results by using Galaxy Evolution Explorer (GALEX) UV data and kinematics taken from the Geneva-Copenhagen Survey for the stars in the sample. Finally, we present a compiled catalog with kinematics and activities for 2529 stars and a list of potential moving group members selected based on their stellar activity level.

Key words. stars: activity – stars: kinematics

1. Introduction

Moving groups (MGs from now on) are groups of stars distributed across the sky that share the same velocity components and form streams. Unlike open clusters, they have no spatial or overdensity center discernible from the field stars. Since the stars that belong to these streams have the same motion, MGs are often called kinematic structures. The study of these structures has a long history (see Zuckerman & Song 2004 for an introduction), but the modern era of MG studies began thanks mainly to the work of Olin Eggen (Eggen 1958). Nowadays, astronomers using data from large surveys like Hipparcos (Perryman et al. 1997; van Leeuwen 2007) have robustly confirmed the existence of MGs (Dehnen 1998). The origin of MGs is still a question of some debate because a fairly large sample of stars is needed to confirm the presence of MGs and also because of the difficulty in identifying the membership of individual stars to these stellar structures.

The two main hypotheses that try to explain the origin of MGs are that either these structures are formed through dynamic interactions, or they have a cluster origin. The first theory postulates that the interaction between field stars and higher density zones (e.g., spiral arms, the galactic bar) produces an overdensity in velocity space, thus creating an MG. Evidence in favor of the dynamic or resonant origin of MGs is the success of computational models in reproducing some of the overdensities seen in velocity space (Dehnen 2000; De Simone et al. 2004a; Antoja et al. 2008; Bovy & Hogg 2010, among others) and the differences in age (Famaey et al. 2008) of individual members that belong to these structures.

The second theory states that when the gas cloud that gives rise to a cluster or stellar association is cleared by winds and/or outflows driven by massive stars, some of the stars that belong to these structures are less affected by the gravitational force of the

system. These stars could eventually become unbound through disk heating processes and leave their initial home. However, they conserve the velocity of the stellar system where they were born producing the streams observed in the sky that we called MGs. So far, the only MG that has been proven to have a cluster origin through an abundance study is HR 1614 (De Silva et al. 2007), and at least a fraction of the stars that are members of the Hyades stream (de Silva et al. 2011, Pompéia et al. 2011).

To shed some light onto this matter, we investigated the stellar activity level and kinematics of the stars in the sample of Jenkins et al. (2011) as well as the relationship between field stars and those towards the centers of known MGs.

2. Activity estimators

2.1. Optical data

For F, G, and K dwarfs a good indicator of activity is the Caɪɪ H and K lines at 3968.5 Å and 3933.7 Å, respectively. If the level of activity in the star is high, the H and K lines consist of a narrow emission component superimposed on the broad absorption line. The ratio between the chromospheric emission lines and the total bolometric emission of the star gives the activity index R'_{HK} (Noyes et al. 1984).

In order to study these kinematic structures known as MGs, it is necessary to have the largest possible sample. With that objective in mind, we merged the Caɪɪ activity index catalogs of Duncan et al. (1991), Henry et al. (1996), Gray et al. (2003), Gray et al. (2006), and Jenkins et al. (2011). In the case of Duncan et al. (1991) catalog, we used the Noyes et al. (1984) calibration to convert the measured S index to $\log R'_{HK}$ values.

For the stars in common, Jenkins et al. (2008) found a discrepancy between their activity values and the ones computed by Gray et al. (2006). This can probably be explained by the use of different calibration stars between the samples. In Jenkins et al.

---

[*] Full Table 1 will be only available in electronic form at the CDS.

Table 1. First ten lines of the full sample of 2529 stars. This catalogue will be available on line.

Star	$U(km/s)$	$V(km/s)$	$W(km/s)$	$\log R'_{HK}$
HD 23	40.00	−22.00	−16.00	−4.780[3]
HIP 72	−48.95	−98.00	19.87	−5.090[1]
HD 105	−10.00	−21.00	−1.00	−4.360[3]
HD 142	−58.00	−38.00	−16.00	−4.703[2]
HD 166	−15.00	−22.00	−10.00	−4.308[2]
HD 361	3.00	2.00	−7.00	−4.684[2]
HD 377	−14.00	−7.00	−4.00	−4.360[4]
HD 400	28.00	−10.00	−8.00	−4.870[4]
HD 564	26.00	4.00	−4.00	−4.830[3]
HIP 599	15.89	11.16	−7.93	−4.990[1]

Notes. Activities from: (1) Jenkins et al. (2011), (2) Gray et al. (2003, 2006), (3) Henry et al. (1996), (4) Wright et al. (2004), (5) Duncan et al. (1991).

Table 2. Centers of known moving groups taken from Antoja et al. (2008) and Montes et al. (2001).

Group name	$U(km/s)$	$V(km/s)$
Pleiades	−12	−22
Hyades	−40	−20
Sirius/UMa	9	3
Coma Berenices	−10	−5
NGC 1901	−25	−10
HR 1614	15	−60
Dehnen 7	20	−20
Dehnen 8	−40	−50
Dehnen 9	−25	50
Dehnen 10	50	0
Dehnen 11	50	−25
IC 2391	−20.8	−15.9
Dehnen 13	−70	−10
Dehnen 14	−70	50
61 Cygni	−80	−53
ζ Herculis	−30	−50
Wolf 630	25.8	−33
Castor	−10.7	−8.0

(2011), this offset was computed to be -0.15 dex, so we proceeded to add +0.15 dex to the $\log R'_{HK}$ obtained by Gray et al. (2003) and Gray et al. (2006).

Jenkins et al. (2008, 2011) presents a spectroscopic study of F,G, and K dwarfs and subgiant stars in the southern hemisphere and computed radial, rotational ($v \sin i$), and galactocentric velocities (U,V,W) as well as the Caɪɪ activity index $\log R'_{HK}$ for stars in the sample. For our analysis we used 865 stars from Jenkins et al. (2011). The other stellar activity catalogs do not have kinematic information and in order to obtain U,V,W velocities, a cross-match between the different catalogs and the Geneva-Copenhagen Survey (GCS, Nordström et al. 2004) was made. In the end, 1000 stars from the combined catalogs of Gray et al. (2003) and Gray et al. (2006), as well as 790, 649, and 292 stars from Henry et al. (1996), Wright et al. (2004), and Duncan et al. (1991), respectively, had GCS velocities.

All the catalogs are unbiased in their selection criteria: Duncan et al. (1991) measured everything observable with their instrument down to V= 12.4 mag; Henry et al. (1996) selected G dwarfs based on their color; Gray et al. (2003 and 2006) selected dwarfs and giants earlier than M0 within 40pc of the Sun; and Jenkins et al. (2011) selected stars based on their color.

Leaving out the stars in common among the samples and removing 99 spectroscopic binaries found using SIMBAD[1], the final data set used in this analysis is composed of 2529 F, G, and K stars with complete stellar activity indices and kinematics. The compilation of catalogs with data for 2529 stars used in this paper will be available on-line for future use (Table 1). The centers of known moving groups used in this work (Table 2) were taken from Antoja et al. (2008), except Castor which was taken from Montes et al. (2001).

Of the final sample of 2529 stars, 2502 have a B-V color index measured by Hipparcos. Using this information, 632 stars can be classified as F stars ($(B − V) < 0.58$), 1577 as G stars ($0.58 < (B − V) < 0.81$), and 293 as K stars ($(B − V) > 0.81$). Hence, G stars are the dominant spectral type in the sample. From the catalog of López-Santiago et al. (2009), 153 stars of our sample are classified as MG members; and from Torres et al. (2006) 134 stars share the same status.
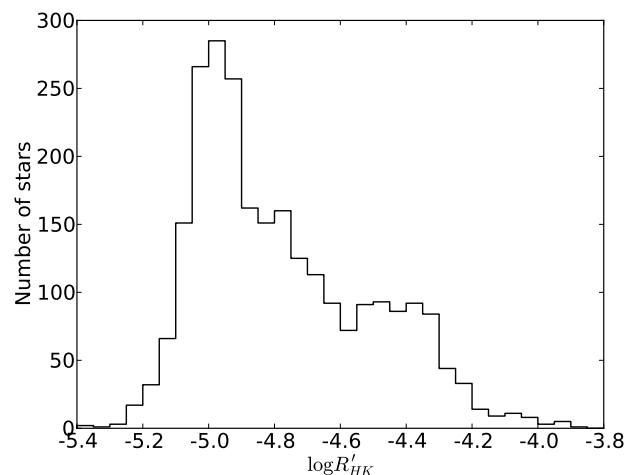
[1] http://simbad.u-strasbg.fr/simbad/

Fig. 1. Chromospheric activity index distribution for the entire sample.

Figure 1 shows the distribution of chromospheric activity for the entire sample. The distribution presents a bimodal feature with peaks representing active stars at ∼ −4.4 dex and inactive stars at ∼ −5.0 dex, in agreement with previous results (Duncan et al. 1991 Henry et al. 1996; Gray et al. 2006; Jenkins et al. 2006). The region in the $\log R'_{HK}$ distribution for solar-type dwarfs and subgiants that is located between the bimodal active and inactive peaks in this distribution is known as the Vaughan-Preston (VP) gap. Older and inactive stars are located beyond this gap with much lower activity and so can serve as a good proxy for younger stars. For descriptions of the VP gap region we refer the reader to other works (e.g., Vaughan & Preston 1980; Baliunas et al. 1995; Henry et al. 1996; Jenkins et al. 2011).
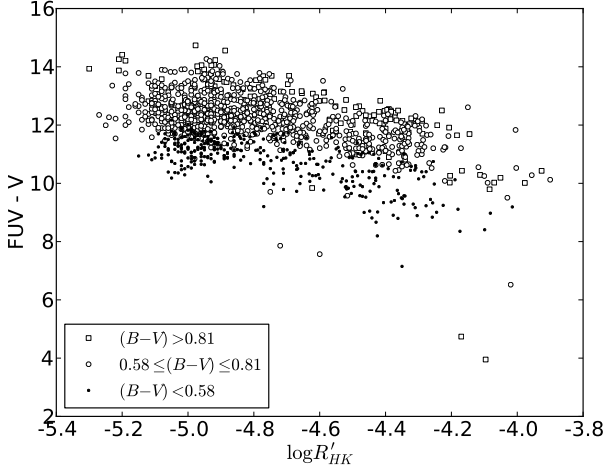
Fig. 2. FUV - V versus $\log R'_{HK}$ for a sub-sample of 1360 stars.

2.2. UV data

Since the UV flux has been shown to be correlated with chromospheric activity, as an extra test of our results we obtained UV photometry using the GALEX All-Sky Survey (Martin et al. 2005) for the entire data set. GALEX ultraviolet bands, far-UV (FUV, 1350 - 1780Å) and near-UV (NUV, 1780 - 2830Å), were acquired by doing a search for the nearest source around the Hipparcos coordinates with a search radius of 10 arcsec. To have a distance-independent indicator, we computed the FUV - V color using Hipparcos photometry. Findeisen et al. (2011) have shown that the color FUV - V is roughly correlated with the calcium HK index (see Fig. 2) and age. From our total sample of 2529 stars, only 1360 had FUV and V magnitudes.

3. Results

3.1. Data analysis

We plotted the contour levels of the U,V,$\log R'_{HK}$ distribution for the data set in order to detect the structures that presented higher levels of stellar activity in kinematic velocity space. To confirm the detection of active regions we created a grid of boxes of 5 km/s in size in U,V (~2σ precision in space velocity of Jenkins et al. 2011) and proceeded to compute the average activity level inside the box. Figure 3 shows the activity index contours versus velocity space for the entire sample (left) and a zoom of the region with the highest density of stars (right); the level of transparency indicates the density number inside each box which is normalized to the box with the highest number of stars in the data set. From the figure we can see that some centers of known moving groups are near regions with active stars.

In Table 3 we present the mean and standard deviation of the stellar activity inside boxes that contain the center of MGs with more than three stars. According to our grid, one box contained the centers of two MGs, Coma Berenices and Castor, which is not surprising given their proximity and the resolution of our grid.

Six of the groups analyzed here present an average activity level between -4.75 and -4.1 dex which is considered to be the active subset (Henry et al. 1996); the rest are considered inactive. The active MGs are consistent with the cluster related origin, since these are also the youngest MGs (Montes et al. 2001). The inactive groups (Dehnen 7, 9, 10, 11, and ζ Herculis) present a

Table 3. Average stellar activity of MGs inside boxes with more than three stars.

Group name	$\log R'_{HK}$	σ_{dev}	N_{stars}
Pleiades	−4.66	0.27	24
Hyades	−4.66	0.24	25
Sirius/UMa	−4.61	0.27	9
Coma Berenices + Castor	−4.59	0.25	15
NGC 1901	−4.53	0.16	11
IC 2391	−4.58	0.26	21
Dehnen 7	−4.81	0.25	9
Dehnen 9	−4.86	0.23	6
Dehnen 10	−4.78	0.19	5
Dehnen 11	−4.86	0.18	4
ζ Herculis	−4.87	0.22	6
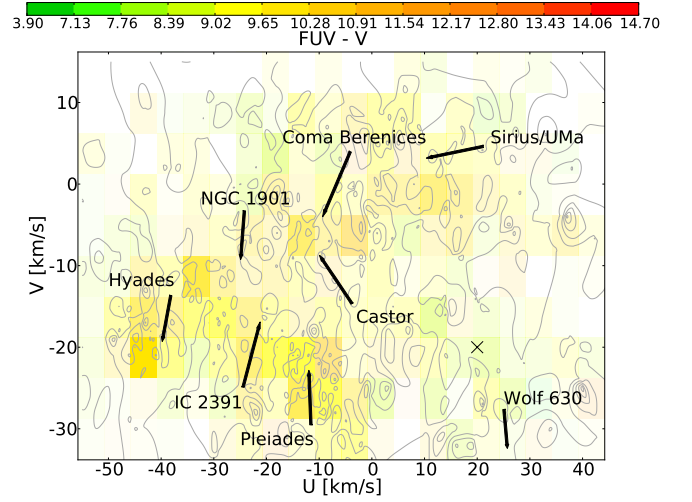
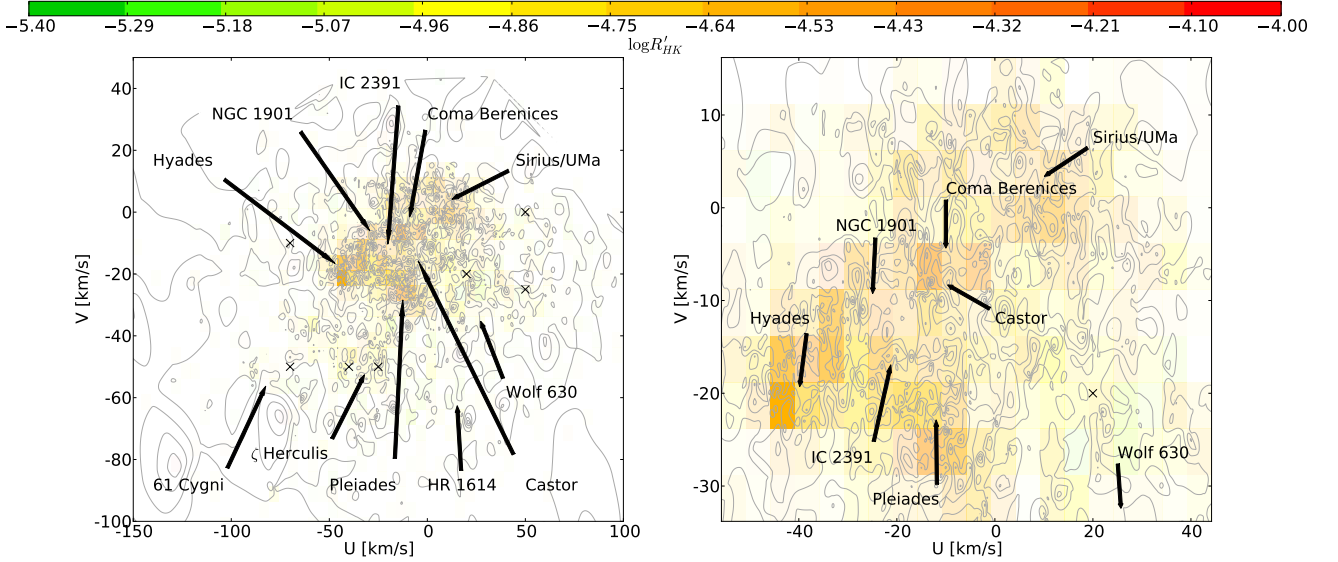
Fig. 4. Plot of the (U,V) region where a higher density of stars is found. Contour levels and grid of the FUV-V for a sample of 1360 stars are shown.

$\log R'_{HK}$ in the range −4.78 - −4.86 and according to the activity-age relation of Mamajek & Hillenbrand (2008), these MGs have ages between 3.0 and 4.1 Gyr.

The same analysis was done on the FUV-V color, and the result (Fig. 4) is very similar to the one found with the activity index, which was expected since the FUV-V is correlated with $\log R'_{HK}$.

3.2. Statistical tests

In order to test the robustness of our claim that areas around MGs in kinematic velocity space generally host more active stars, we ran some bootstrap simulations to generate random data sets drawn from the observed data to test how often the MG centers would appear to host inactive boxes at our grid resolution. This allowed us to test how often randomness would give rise to these results in our data. To do this, we randomly scrambled the mean activities of our boxes to generate fake data sets, but crucially, only used boxes that contain at least three stars, which is necessary to ensure as best we can that we are not biasing our data through small random fluctuations because of low number statistics. We ran the bootstrap simulation 500000 times to ensure a high level of statistical significance in our final probabilities.

Fig. 3. Plot of the (U,V) velocity space showing contour levels of stellar activity ($\log R'_{\rm HK}$) and the grid of boxes for the sample (left). The right panel shows a zoom of the central region where a higher density of stars is found. The transparency level indicates the density number of stars inside the boxes. The crosses mark the center of the Dehnen 7, 8, 9, 10, 11, 13, 14 groups.

We decided to test our data set in three different ways: a) the fraction of MG boxes that are more active than the VP region ($\log R'_{\rm HK} > -4.70$) versus the inactive boxes, b) the ratio between this first MG fraction (MG_{VP}) and the same fraction for field boxes, and c) the ratio between the mean activity of boxes in MGs compared with the same mean activity for boxes in the field.

The bootstrap results for the first test are shown in Fig. 5a where the normalized frequencies of these ratios are shown and the original observed value is highlighted by the downward pointing arrow. Only 4.58% of scrambled runs were found to host a set of MG boxes with a higher ratio of more active values than the original data set (unshaded area in Fig. 5a).
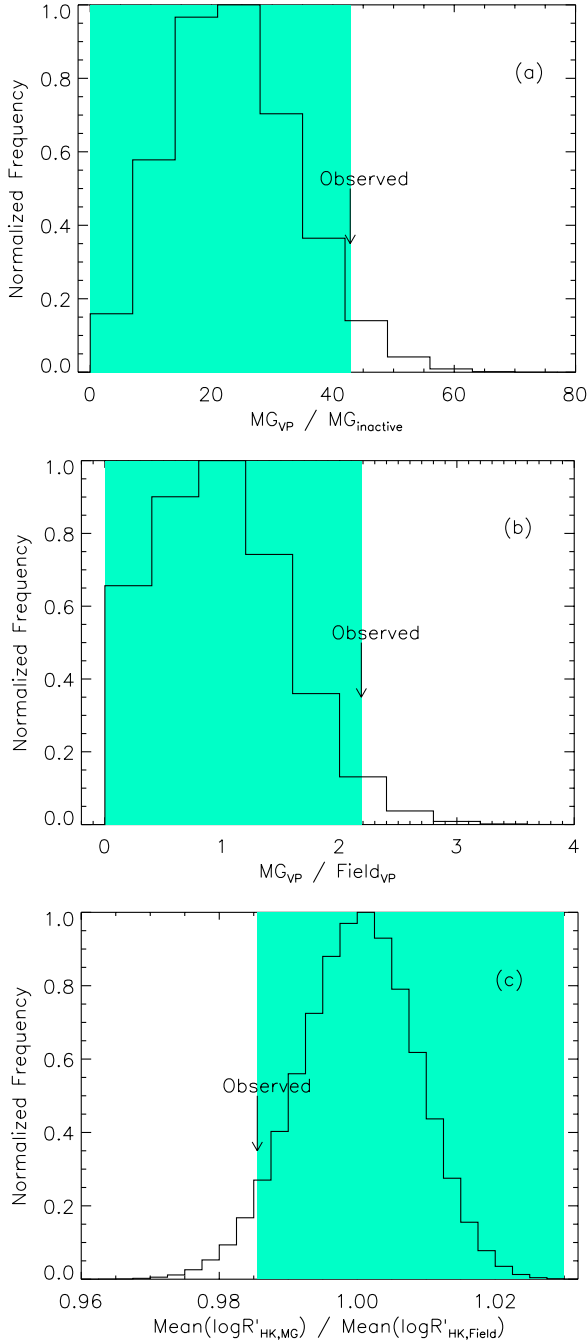
The second test (Fig. 5b), where we compared the fraction of boxes that are more active than the VP region against the field, shows a distribution that appears to be Poissonic. This is not surprising, given that this is essentially based on counting statistics. Again the original observed value is shown by the downward pointing arrow and, as mentioned, we find a similar value of only 4.58% for ratios with more active field stars beyond the VP gap compared to the MGs, meaning we have 95.4% confidence in our results.

The final test we decided to implement was to then compare the overall mean values between the MG boxes and the field boxes in our sample. This provided a robust test across the entire sample and increased the resolution of our bootstrap method given that we were sampling a larger number within our parameter-space. Figure 5c shows the results from this bootstrap analysis, and now we clearly see a Gaussian shape and much better resolution than in the first two tests. Again, the observed value is shown by the downward pointing arrow. This time we find only 4.8% of runs have a higher mean activity in the field compared to the mean activity of the MG centers, a little more than a 2σ result. By focusing on only the youngest MG, and those with the most stars in our grid we could increase the significance of this result, but this would introduce a bias into our methodology, so we have decided to include all known MGs for the time being.

The same bootstrap analysis was performed using the FUV - V color as an activity indicator for the MG boxes (Fig. 6) and we found that in 23.89% of the runs the field stars have a higher stellar activity than the MG. The UV data confirm our results but not at the same level of significance as the $\log R'_{\rm HK}$ index. This is explained because the FUV - V color is only weakly correlated with the calcium index and the relation between these two quantities is not strong; the purpose of using UV data was to have an independent activity indicator of the results found with the $\log R'_{\rm HK}$ index using a large and homogeneous survey like GALEX.

Since stellar chromospheric activity depends on the mass of the star, we performed the same statistical tests separating the stars in the sample by their spectral classification using their (B-V) color index. For F and K stars, the results for the tests are similar: Test a) 74.7% and 64.1% of the time we found boxes with higher activities than the original set; Test b) in 38.5% and 33.3% of the runs, field stars presented a higher activity level than the MG boxes; and Test c) 62.5% and 49.1% of the time the mean activity level of the field surpassed the level of MG boxes. This result contradicts the statistics found by using the full sample (without separating the stars by spectral classification), but we believe this was caused by the low number of F and K stars in our sample (25.3% and 11.7% of the total, respectively). This low number of F and K stars is even more evident when we look at the most populated boxes that contain a known MG, i.e., the Hyades, Pleiades, and IC 2391. Of a total of 25 stars in the box containing the Hyades, only 8 and 2 stars are F and K types; for Pleiades, of 24 stars only 4 and 6 are F and K, respectively; and finally, for IC 2391 only 7 and 1 stars have (B-V) color indices consistent with F and K spectral types. The low number of F and K stars in our sample affects the estimation of the stars that are more active than the VP gap for test a) and the level of activity of the field for tests b) and c), in the sense that there are fewer boxes with more than three stars to compute the mean level of $\log R'_{\rm HK}$. This produces contradictory results when compared with the full sample and with the results found using only G stars.
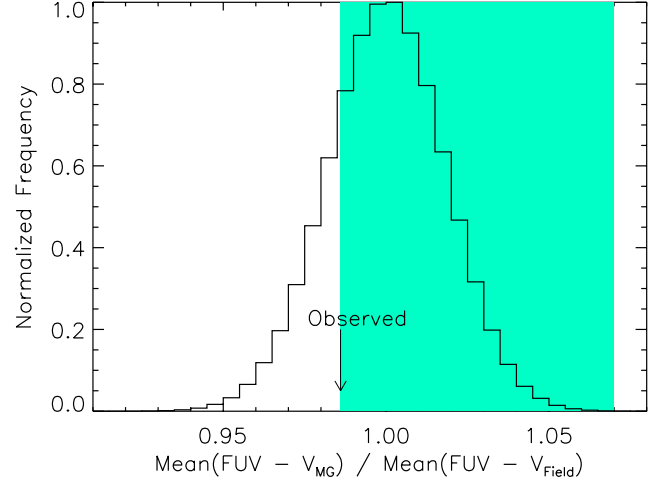
For G stars, the results for the different tests are: 24.1%, 6.2%, and 15.9% for tests a), b), and c), respectively. This is

Fig. 6. Similar to Fig. 5c, bootstrap simulation test showing the ratio between the mean FUV - V color of boxes that host MGs compared with the boxes in the field.

rating the stars by spectral type, we find that MG regions in kinematic space are generally more active than in the field at around the 2σ level, reinforcing the hypothesis that, in general, most of these kinematic regions are actual overdensities of young stars and so are true MGs and not dynamic resonances attributed to structures in the galactic disk of our galaxy.

3.3. Candidates

In Table 4 we present a list of active stars ($\log R'_{HK} \geq -4.70$) that belong to the boxes in the grid that contained the center of a known MG. Of our list of candidates, HD 206860, HD 142415, HD 13507, HD 40979, and HD 73256 have known low mass companions or planets. Some of the stars presented here are classified as possible members of MGs by previous studies (e.g., Montes et al. 2001, López-Santiago et al. 2006, Maldonado et al. 2010, Nakajima & Morino 2012). A total of 42 stars are not cataloged and they could be new MG members.

4. Discussion

Based on our data sample, the statistical tests favor the idea that the MGs have a higher fraction of active stars than the field. Given our current theories of stellar formation and evolution, it is expected that young stars present a higher activity level when compared with older stars. This implies that at least a significant part of the stars that belong to these structures must be relatively young and since they are occupying the same velocity space, it is highly likely that they have the same origin.

The mean survival time of an MG is $\sim$ 1 Gyr before being dispersed by disk heating mechanisms (De Simone et al. 2004b); according to the activity-age relation from Mamajek & Hillenbrand (2008) a star with an age of 1 Gyr should have a calcium activity index of approximately -4.56. From our results, the MGs that have an age similar to 1 Gyr are Pleiades, Hyades, Sirius/UMa, Coma Berenices, Castor, NGC 1901, and IC 2391. All of these MGs are known to be young, with ages less than 1 Gyr (Montes et al. 2001), so a higher chromospheric activity level was expected. The groups Dehnen 7, 9, 10, 11, and ζ Herculis present ages ranging from 3 to 4.1 Gyr, but even if they are older than the canonical disruption time scale, according to

Fig. 5. Bootstrap simulation tests of our data set: a) test the fraction of MG boxes that are more active than the VP region, b) the ratio between this first MG fraction and the same fraction for field boxes and c) the ratio between the mean activity of boxes in MGs compared with the same mean activity for boxes in the field. The original observed values are highlighted by the downward pointing arrows and the green shaded areas represent the percentage of times where the MG boxes showed a higher level of activity for each test.

more in line with the results found by using the full sample, which was expected since the sample is dominated by G stars (63% of the total).

Given these three tests made with $\log R'_{HK}$ for the entire sample, the one performed with the FUV - V color index, and sepa-

our results they also have a higher stellar activity level when compared to the field stars that are near the center of the MG. In other words, the old MGs also conserve a signature showing that those stars are somehow related because they have an activity level higher than their environment and share the same velocity.

In the case that these structures are indeed formed by dynamic or resonant interactions, one would expect that the stars that composed the system would have different origins and hence different stellar parameters such as metallicity. Several studies have shown that the stars that belong to MGs have a wide spread of chemical compositions as opposed to an open cluster (e.g., Bensby et al. 2007; Antoja et al. 2008), but this could be caused by contamination in the selection of stars.

Given our results, we think that the calcium activity index could be used as a parameter to pre-select stars as candidate MG members, which would then be confirmed through an abundance study. We plan to study the abundances of the active MG stars from the Jenkins et al. (2011) sample; metallicities are currently being processed for the entire data set. However, we note that generally high activity means high rotation and therefore a higher fraction of blended lines in stellar spectra, which leads to less robust atomic abundance measurements.

5. Conclusions and future work

We have presented a stellar activity study of moving groups using a sample of 2529 stars. By creating a grid of boxes in (U,V) velocity space and taking the mean activity inside the boxes, we find that, on average, the moving groups present a higher level of stellar activity than the field stars do. We find a similar result, although with a less statistical significance, by repeating the procedure with ultraviolet data taken from GALEX and for the G stars in the sample. Finally, a list of possible MG members with a high level of stellar activity is presented. We speculate that if this higher level of chromospheric activity in MG is a consequence of the fact that these structures are mainly composed of young stars, this is strong evidence that stars that belong to these streams form a real physical structure, that they have a common origin, and that they are not structures formed by resonance interactions.

We plan to follow-up these MG members, and those in the literature, with high-contrast adaptive optics (AO) imaging techniques to hunt for orbiting sub-stellar companions. In particular, we shall focus on the lowest-mass MG members, the later M-types (e.g., Clarke et al. 2010; Gálvez-Ortiz et al. 2010), where current AO imaging can reach down into the Jupiter-mass regime. Late-type M-dwarfs are soon to provide large increase in the number of low-mass planets because methods and techniques are being pushed to hunt for such planets using the radial velocity and transit method (Nutzman & Charbonneau 2008; Ramsey et al. 2008; Jenkins et al. 2009; Barnes et al. 2012). However, such techniques are biased toward the oldest, most quiescent stars, and therefore direct imaging of young MG members can help to extend the parameter space in the search for planetary-mass objects around the lowest-mass stars.

References

Antoja, T., Figueras, F., Fernández, D., & Torra, J. 2008, A&A, 490, 135
Baliunas, S. L., Donahue, R. A., Soon, W., Gilliland, R., & Soderblom, D. R. 1995, in Bulletin of the American Astronomical Society, Vol. 27, American Astronomical Society Meeting Abstracts #186, 839–+
Barnes, J. R., Jenkins, J. S., Jones, H. R. A., et al. 2012, MNRAS, 424, 591
Bensby, T., Oey, M. S., Feltzing, S., & Gustafsson, B. 2007, ApJ, 655, L89
Boesgaard, A. M. & Budge, K. G. 1988, ApJ, 332, 410
Bovy, J. & Hogg, D. W. 2010, ApJ, 717, 617
Clarke, J. R. A., Pinfield, D. J., Gálvez-Ortiz, M. C., et al. 2010, MNRAS, 402, 575
De Silva, G. M., Freeman, K. C., Bland-Hawthorn, J., Asplund, M., & Bessell, M. S. 2007, AJ, 133, 694
de Silva, G. M., Freeman, K. C., Bland-Hawthorn, J., et al. 2011, MNRAS, 415, 563
De Simone, R., Wu, X., & Tremaine, S. 2004a, MNRAS, 350, 627
De Simone, R., Wu, X., & Tremaine, S. 2004b, MNRAS, 350, 627
Dehnen, W. 1998, AJ, 115, 2384
Dehnen, W. 2000, AJ, 119, 800
Duncan, D. K., Vaughan, A. H., Wilson, O. C., et al. 1991, ApJS, 76, 383
Eggen, O. J. 1958, MNRAS, 118, 65
Famaey, B., Siebert, A., & Jorissen, A. 2008, A&A, 483, 453
Findeisen, K., Hillenbrand, L., & Soderblom, D. 2011, AJ, 142, 23
Gálvez-Ortiz, M. C., Clarke, J. R. A., Pinfield, D. J., et al. 2010, MNRAS, 409, 552
Gray, R. O., Corbally, C. J., Garrison, R. F., et al. 2006, AJ, 132, 161
Gray, R. O., Corbally, C. J., Garrison, R. F., McFadden, M. T., & Robinson, P. E. 2003, AJ, 126, 2048
Henry, T. J., Soderblom, D. R., Donahue, R. A., & Baliunas, S. L. 1996, AJ, 111, 439
Jenkins, J. S., Jones, H. R. A., Pavlenko, Y., et al. 2008, A&A, 485, 571
Jenkins, J. S., Jones, H. R. A., Tinney, C. G., et al. 2006, MNRAS, 372, 163
Jenkins, J. S., Murgas, F., Rojo, P., et al. 2011, A&A, 531, A8+
Jenkins, J. S., Ramsey, L. W., Jones, H. R. A., et al. 2009, ApJ, 704, 975
Khodjachikh, M. F. & Romanovsky, E. A. 2000, Kinematika i Fizika Nebesnykh Tel, 16, 20
López-Santiago, J., Micela, G., & Montes, D. 2009, A&A, 499, 129
López-Santiago, J., Montes, D., Crespo-Chacón, I., & Fernández-Figueroa, M. J. 2006, ApJ, 643, 1160
Makarov, V. V. & Urban, S. 2000, MNRAS, 317, 289
Maldonado, J., Martínez-Arnáiz, R. M., Eiroa, C., Montes, D., & Montesinos, B. 2010, A&A, 521, A12
Mamajek, E. E. & Hillenbrand, L. A. 2008, ApJ, 687, 1264
Martin, D. C., Fanson, J., Schiminovich, D., et al. 2005, ApJ, 619, L1
Montes, D., López-Santiago, J., Gálvez, M. C., et al. 2001, MNRAS, 328, 45
Nakajima, T. & Morino, J.-I. 2012, AJ, 143, 2
Nordström, B., Mayor, M., Andersen, J., et al. 2004, A&A, 418, 989
Noyes, R. W., Hartmann, L. W., Baliunas, S. L., Duncan, D. K., & Vaughan, A. H. 1984, ApJ, 279, 763
Nutzman, P. & Charbonneau, D. 2008, PASP, 120, 317
Perryman, M. A. C., Lindegren, L., Kovalevsky, J., et al. 1997, A&A, 323, L49
Pompéia, L., Masseron, T., Famaey, B., et al. 2011, MNRAS, 415, 1138
Ramsey, L. W., Barnes, J., Redman, S. L., et al. 2008, PASP, 120, 887
Soubiran, C. & Girard, P. 2005, A&A, 438, 139
Torres, C. A. O., Quast, G. R., da Silva, L., et al. 2006, A&A, 460, 695
van Leeuwen, F. 2007, A&A, 474, 653
Vaughan, A. H. & Preston, G. W. 1980, PASP, 92, 385
Wright, J. T., Marcy, G. W., Butler, R. P., & Vogt, S. S. 2004, ApJS, 152, 261
Zuckerman, B., Bessell, M. S., Song, I., & Kim, S. 2006, ApJ, 649, L115
Zuckerman, B. & Song, I. 2004, ARA&A, 42, 685

Table 4. Potential moving group members.

HD	RA (J2000.0)	DEC (J2000.0)	U [km/s]	V[km/s]	W[km/s]	log R'_{HK}
		Pleiades				
HD 166[1],[2],[4]	00 06 36.7	+29 01 17.4	-15.0	-22.0	-10.0	-4.30
HD 17925[2],[3]	02 52 32.1	-12 46 10.9	-15.0	-21.0	-9.0	-4.20
HD 26864	04 12 43.7	-47 33 56.5	-14.4	-23.0	-13.9	-4.47
HD 37394[1],[2]	05 41 20.3	+53 28 51.8	-13.0	-23.0	-14.0	-4.40
HD 38397	05 43 35.8	-39 55 24.7	-11.0	-21.0	-6.0	-4.26
HD 48286	06 42 05.2	-15 12 54.9	-14.0	-22.0	-34.0	-4.62
HD 100563[1]	11 34 21.9	+03 03 36.5	-14.0	-21.0	-8.0	-4.52
HD 116386[4]	13 24 03.7	-45 14 14.2	-13.5	-23.6	-1.0	-4.40
HD 130307	14 47 16.1	+02 42 11.6	-15.0	-23.0	6.0	-4.52
HD 202575[1],[3],[4]	21 16 32.4	+09 23 37.7	-11.0	-20.0	-4.0	-4.37
HD 206860[1],[2],[4]	21 44 31.3	+14 46 18.9	-14.6	-21.5	-10.8	-4.42
HD 220117	23 20 53.2	+38 10 56.3	-15.0	-21.0	-16.0	-4.51
		Hyades				
HD 3196	00 35 14.8	-03 35 34.2	-36.0	-19.0	-13.0	-4.31
HD 5133[3]	00 53 01.1	-30 21 24.9	-36.0	-20.0	13.0	-4.60
HD 28406[5]	04 29 30.3	+17 51 47.3	-40.0	-19.0	-1.0	-4.46
HD 40979	06 04 29.9	+44 15 37.5	-37.0	-21.0	8.0	-4.63
HD 61033	07 34 28.0	-52 58 05.3	-38.1	-22.6	4.9	-4.42
HD 62911	07 44 47.1	-33 43 54.3	-37.0	-22.0	-3.0	-4.47
HD 73256	08 36 23.0	-30 02 15.4	-36.0	-21.0	-15.0	-4.52
HD 87978[4]	10 08 26.5	-11 06 54.7	-37.6	-23.2	0.9	-4.45
HD 92855	10 44 00.6	+46 12 23.9	-40.0	-21.0	-14.0	-4.44
HD 106489[6]	12 14 57.4	-41 08 21.9	-38.0	-23.0	-18.0	-4.48
HD 111998	12 53 11.1	-03 33 11.1	-36.0	-20.0	-6.0	-4.43
HD 132301	14 59 45.0	-43 48 40.8	-39.0	-23.0	-8.0	-4.35
HD 140011	15 43 11.8	-44 43 12.3	-38.0	-19.0	-7.0	-4.46
HD 153330[6]	17 00 25.4	-37 56 14.0	-36.0	-19.0	19.0	-4.64
HD 215532	22 47 06.7	-60 04 33.2	-40.0	-22.0	-4.0	-4.68
		Sirius/UMa				
HD 25926[6]	04 04 55.9	-35 26 47.6	8.0	3.0	-10.0	-4.45
HD 30059	04 43 47.7	-12 17 40.0	5.2	1.6	1.0	-4.60
HD 152388	16 56 52.1	-60 57 24.6	8.0	5.0	4.0	-4.62
HD 187532	19 50 46.7	-10 45 48.6	5.0	5.0	3.0	-4.09
HD 215657[6]	22 47 26.7	-44 57 54.5	9.0	2.0	-7.0	-4.28
		Coma Berenices + Castor				
HD 8907	01 28 34.3	+42 16 03.6	-10.0	-4.0	-17.0	-4.50
HD 10611[6]	01 43 14.3	-21 37 11.1	-7.0	-7.0	-8.0	-4.30
HD 13507[1],[4]	02 12 55.0	+40 40 06.0	-9.0	-6.0	-11.0	-4.39
HD 13531	02 13 13.3	+40 30 27.3	-10.0	-6.0	-11.0	-4.34
HD 18809[6]	03 00 19.7	-37 27 16.1	-9.0	-4.0	-10.0	-4.33
HD 21175	03 23 35.2	-40 04 34.9	-8.0	-7.0	-10.0	-4.62
HD 21722[7]	03 25 36.2	-69 20 11.1	-7.0	-7.0	-15.0	-4.31
HD 25120	03 55 18.3	-65 17 05.0	-9.0	-5.0	-13.0	-4.40
HD 33256[8]	05 08 43.7	-04 27 22.3	-10.0	-6.0	2.0	-4.61
HD 103978	11 58 19.5	-55 14 22.4	-8.4	-5.1	-8.5	-4.46
		NGC 1901				
HD 7678	01 15 45.0	-53 42 56.4	-25.0	-11.0	1.0	-4.70
HD 10655	01 43 32.3	-19 24 12.6	-24.4	-9.4	-6.41	-4.44
HD 30157	04 44 33.8	-16 03 54.1	-21.6	-11.1	-3.9	-4.67
HD 43162[1],[3],[4]	06 13 45.2	-23 51 42.9	-21.0	-10.0	-7.0	-4.33
HD 57852[9]	07 20 21.5	-52 18 43.2	-22.0	-13.0	-8.0	-4.16
HD 84273	09 43 20.2	-29 48 14.4	-22.0	-10.0	-5.0	-4.50
HD 118036	13 34 16.2	-00 18 49.6	-23.0	-12.0	0.0	-4.57
HD 142415[6]	15 57 40.7	-60 12 00.9	-24.0	-13.0	1.0	-4.62
HD 162396[8]	17 52 52.5	-41 59 47.4	-24.0	-11.0	-32.0	-4.64
HD 218168	23 04 02.1	+74 28 38.7	-25.0	-9.0	-2.0	-4.50
		IC 2391				
HD 25680[1],[3]	04 05 20.2	+22 00 32.0	-25.0	-14.0	-6.0	-4.45
HD 53143[1],[4]	06 59 59.6	-61 20 10.2	-25.0	-18.0	-15.0	-4.39
HD 61005	07 35 47.4	-32 12 14.0	-22.0	-14.0	-4.0	-4.18
HD 62850[6],[10]	07 42 36.0	-59 17 50.7	-25.0	-18.0	-2.0	-4.27
HD 62848[9],[10]	07 43 21.4	-52 09 50.7	-25.0	-18.0	-3.0	-4.33
HD 103742[4],[10]	11 56 42.3	-32 16 05.4	-24.0	-18.0	-4.0	-4.33
HD 110419	12 42 08.8	-31 49 10.6	-21.1	-18.1	-16.2	-4.48

Table 4. continued.

HD	RA (J2000.0)	DEC (J2000.0)	U [km/s]	V[km/s]	W[km/s]	log R'_{HK}
HD 113553[6]	13 05 16.8	-50 51 23.8	-23.0	-17.0	2.0	-4.30
HD 120352[4]	13 48 58.1	-01 35 34.6	-21.2	-18.5	-10.0	-4.64
HD 151598	16 50 46.8	-49 12 39.3	-25.0	-15.0	-8.0	-4.40
HD 158866	17 47 42.6	-82 12 59.1	-25.0	-17.0	-4.0	-4.35
HD 200361	21 04 31.2	-44 27 42.4	-22.4	-17.9	-11.8	-4.59
HD 203030[4]	21 18 58.2	+26 13 49.9	-23.0	-16.0	-12.0	-4.37
Dehnen 7						
HD 8326	01 22 07.6	-26 53 35.1	24.0	-23.0	-22.0	-4.65
HD 21899	03 30 13.5	-41 22 11.7	20.0	-23.0	-13.0	-4.60
HD 137778[3]	15 28 12.2	-09 21 28.2	22.0	-22.0	-20.0	-4.32
Dehnen 9						
HD 11683	01 54 22.1	-15 43 26.3	-24.1	-51.5	8.8	-4.46
HD 73744	08 32 15.5	-76 55 43.6	-22.0	-50.0	-31.0	-4.68
Dehnen 10						
HD 64184	07 49 26.6	-59 22 51.0	52.0	-2.0	28.0	-4.63
HD 71251	08 26 11.9	-05 45 05.4	50.3	-0.2	-6.1	-4.58
HD 192117	20 20 24.1	-75 34 40.3	52.0	0.0	4.0	-4.67
Dehnen 11						
HD 37962	05 40 51.9	-31 21 03.9	54.0	-24.0	-26.0	-4.627
ζ Herculis						
HD 59984[8]	07 32 05.7	-08 52 52.7	-29.0	-51.0	-18.0	-4.51

Notes. (1) Nakajima & Morino (2012); (2) López-Santiago et al. (2006); (3) Maldonado et al. (2010); (4) Montes et al. (2001); (5) Boesgaard & Budge (1988); (6) Torres et al. (2006); (7) Khodjachikh & Romanovsky (2000); (8) Soubiran & Girard (2005); (9) Makarov & Urban (2000); (10) Zuckerman et al. (2006).